Received Date : 05-Jul-2016

Revised Date : 23-Aug-2016

Accepted Date : 26-Aug-2016

Article type : Technical Advance

Generation of chromosomal deletions in dicotyledonous plants employing a user-friendly genome editing toolkit

Authors:

Jana Ordon[1], Johannes Gantner[1], Jan Kemna[1], Lennart Schwalgun[1], Maik Reschke[1,2], Jana Streubel[1,2], Jens Boch[1,2], Johannes Stuttmann[1*]

Affiliation: [1] Department of Genetics, Martin Luther University Halle (Saale), Weinbergweg 10, 06120 Halle, Germany

email: JO jana.ordon@gmx.de; JG johannes.gantner@genetik.uni-halle.de; JK JannKemna@gmx.de; Lennart-Schwalgun@web.de; JStr jana.streubel@genetik.uni-hannover.de; MR maik.reschke@genetik.uni-hannover.de; JB jens.boch@genetik.uni-hannover.de; JStu johannes.stuttmann@genetik.uni-halle.de

Suggested running title: Cas9 for chromosomal deletions

Keywords: CRISPR/Cas, chromosomal deletion, *Nicotiana benthamiana*, *Arabidopsis thaliana*, plant immunity, EDS1

Significance statement (max 75 words, revised by editorial office):
In plants, genome editing has mostly been used to generate point mutations, but deletion alleles are often desirable. Here, we developed a toolkit for simple and efficient assembly of genome editing constructs and used it to generate deletions in both *Nicotiana benthamiana* and Arabidopsis. Small deletions (< 100 bp) were recovered with relatively high frequencies in both species, while large deletions (up to 120 kb) were less frequent.

[*] corresponding author:

Johannes Stuttmann (johannes.stuttmann@genetik.uni-halle.de); address as indicated above, Telephone +49-345-5526345, fax +49-345-5527151

[2] Present address: Department of Plant Biotechnology, Leibniz University Hannover, Herrenhäuser Str. 2, 30419 Hannover, Germany

SUMMARY

Genome editing facilitated by Cas9-based RNA-guided nucleases (RGNs) is becoming an increasingly important and popular technique for reverse genetics in both model and non-model species. So far, RGNs were mainly applied for the induction of point mutations, and one major challenge consists in the detection of genome-edited individuals from a mutagenized population. Also, point mutations are not appropriate for functional dissection of non-coding DNA. Here, the multiplexing capacity of a newly developed genome editing toolkit was exploited for the induction of inheritable chromosomal deletions at six different loci in *Nicotiana benthamiana* and Arabidopsis. In both species, the preferential formation of small deletions was observed, suggesting reduced efficiency with increasing deletion size. Importantly, small deletions (< 100 bp) were detected at high frequencies in *N. benthamiana* T_0 and Arabidopsis T_2 populations. Thus, targeting of small deletions by paired nucleases represents a simple approach for the generation of mutant alleles segregating as size polymorphisms in subsequent generations. Phenotypically selected deletions of up to 120 kb occurred at low frequencies in Arabidopsis, suggesting larger population sizes for the discovery of valuable alleles from addressing gene clusters or non-coding DNA for deletion by programmable nucleases.

INTRODUCTION

Genome editing refers to the targeted modification of defined positions within a genome using site-specific nucleases. Nuclease-generated double-strand breaks are repaired by non-homologous end-joining (NHEJ) or, in the presence of a repair template, by homology-directed repair (HDR). Error-prone NHEJ commonly creates small genomic deletions or insertions leading to the potential inactivation of a gene product (knock-out), while HDR can mediate the introduction of specific sequences (knock-in). Zinc-finger nucleases were initially used as programmable nucleases for genome editing applications (Kim *et al.* 1996, Townsend *et al.* 2009). A first genome editing revolution was then triggered by the invention of TALENs (Christian *et al.* 2010). TALENs are fusions of the *FokI* nuclease domain to a DNA-binding domain derived from a TAL effector of plant pathogenic *Xanthomonas* bacteria. This DNA-binding domain consists of 34-amino acid repeat modules, which bind to DNA in a one repeat-one nucleotide manner. Nucleotide-specificity is conferred by two hypervariable amino acids at position 12 and 13 in each repeat (Boch and Bonas 2010, Boch *et al.* 2009). Due to the catalytic properties of *FokI*, two TALENs binding a target sequence in appropriate spacing have to be co-expressed to allow dimerization of the nuclease and to generate DSBs (Christian*, et al.* 2010). TALENs binding virtually any sequence with high specificity can be constructed with relative ease (e.g. Geissler *et al.* 2011, Liang *et al.* 2014, Weber *et al.* 2011b), and TALENs were used for modification of both model and crop plant genomes (e.g. Christian *et al.* 2013, Clasen *et al.* 2016, Sosso *et al.* 2015).

Genome editing was further simplified by harnessing RNA-guided nucleases (RGNs) derived from bacterial CRISPR/Cas systems for induction of DSBs (for review, see Doudna and Charpentier 2014, Wiedenheft *et al.* 2012). The Cas9 (CRISPR-associated Protein 9) from *Streptococcus pyogenes* is the most commonly used nuclease, and is in the natural system directed to target sites by a chimeric RNA consisting of crRNA and tracrRNA (Jinek *et al.* 2012). This chimeric RNA species can be collapsed into one molecule, the single guide RNA (sgRNA; Jinek*, et al.* 2012). Cas9 target specificity can thus be reprogrammed by co-expression of different sgRNAs. The sgRNA directs Cas9 to target sites by

complementary base-pairing, but target sites have to be flanked by a protospacer-adjacent motif (PAM; NGG for *Sp*Cas9) in order to be cleaved.

The Cas9 system has been adapted for use in many different plants systems ranging from algae and mosses to monocotyledonous and dicotyledonous plants (Belhaj *et al.* 2015, Bortesi and Fischer 2015, Jiang *et al.* 2014a). In most cases, Cas9-based nucleases are expressed *in planta* from an *Agrobacterium*-delivered T-DNA. This necessitates the construction of complex T-DNAs comprising multiple genes, which may represent a first challenge for potential users. Another challenge consists in the actual selection of mutants from a population of Cas9 and sgRNA(s)-expressing plants. So far, Cas9 was in plants mainly used for induction of point mutations at exemplary loci with associated mutant phenotypes (for review, see Belhaj*, et al.* 2015, Bortesi and Fischer 2015). Here, a toolkit for extremely simple and efficient assembly of RGN-coding constructs was developed and employed for the generation of chromosomal deletions. Deletions of different sizes were induced at six independent loci in *Nicotiana benthamiana* and Arabidopsis, and mutant alleles were isolated either by associated phenotype or PCR screening. Our results show that large deletions up to 120 kb are feasible, but occur at low frequencies. In contrast, small deletions (< 100 bp) can be induced with relatively high frequencies in both Arabidopsis and *N. benthamiana*, and provide a straightforward workflow for mutant identification.

RESULTS

DEVELOPMENT OF A STREAMLINED TOOLKIT FOR GENOME EDITING IN DICOTYLEDONOUS PLANTS

The modular cloning principle and toolbox recently provided to the plant community as a synthetic biology "starter kit" are at the basis of Dicot Genome Editing (pDGE) vectors developed here (Engler *et al.* 2014, Weber *et al.* 2011a). Different types of vectors were generated for streamlined assembly of RGN-encoding constructs (Figure 1a, Table S1). The *Agrobacterium*-mediated transformation-compatible "one step, one nuclease" vectors pDGE62-65 are designated for expression of a single sgRNA together with Cas9 and plant selectable marker (BASTA or kanamycin resistance). Assembly

of an sgRNA transcriptional unit (TU) in pDGE62-65 is achieved in a single step by exchanging a *ccdB* negative selection cassette for two hybridized oligonucleotides in a simultaneous restriction/ligation reaction using *BpiI* (*BbsI*; Figure 1b). "Recipient" vectors have a similar architecture as pDGE62-65, but are designated for multiplexing applications (Figure 1a). In a two-step assembly, sgRNA TUs are first assembled in "sgRNA shuttle vectors", and subsequently mobilized into recipient vectors. The generation of an sgRNA TU in shuttle vectors is carried out as described for the one-step, one nuclease vectors (Figure 1b). Resulting sgRNA TUs are flanked by *BsaI* restriction sites, and generated overhangs vary between shuttle vectors (Figure 1a). Arrays of two, four or eight sgRNA TUs can be assembled in any recipient plasmid by combining it with compatible derivatives of sgRNA shuttle vectors in a simultaneous restriction/ligation reaction using *BsaI* (*Eco31I*, Figure 1c). For simplicity, shuttle vectors were named M1-M8 (for module 1-8) according to their position in an sgRNA array, and modules closing the vector by ligation to the vector overhang received an additional "E" (END; Figures 1b, c). Unique linker sequences were included in modules M1 and M5 to provide primer binding sites for sequence verification of sgRNA arrays (Figure 1c, Appendix S1). Based on the same principle, also nickase recipient (pDGE76-79; equivalent to pDGE1-4, but incorporating Cas9 D10A) and transcriptional activator vectors (Figure 1a, incorporating dCas9 fused to a TAL activation domain) were generated. These materials are made available, but will not be described in detail here.

sgRNA expression is driven by an Arabidopsis U6 promoter (p*At*U6-26) in all vectors. The double *35S* promoter (p35S) coupled with a *nos* terminator and the *Ubi4-2* promoter from parsley (p*Pc*Ubi) coupled with an *ocs* terminator were employed for Cas9 expression in one step, one nuclease vectors and first generation recipient vectors (Figure 1a). The 2x35S:Cas9 expression cassette and p*Pc*Ubi promoter were previously successfully used for genome editing in *N. benthamiana* and Arabidopsis, respectively (Belhaj *et al.* 2013, Fauser *et al.* 2014, Schiml *et al.* 2014). The assembly of first generation recipient vectors integrated the Cas9 expression cassette as a level 1 module of the modular cloning system (Engler*, et al.* 2014, Weber*, et al.* 2011a), allowing simple modification of promoter/terminator sequences. However, this assembly strategy depended on custom modules for the

introduction of plant-selectable markers, and was of limited flexibility (Figure S1a). An improved assembly strategy (Figure S1b) was developed to accommodate additional modules in recipient vectors and achieve higher compatibility with the modular cloning system (Engler*, et al.* 2014, Weber*, et al.* 2011a). Based on this, second generation recipient vectors providing additional promoters for Cas9 expression and selectable markers were generated (Figure 1a). The *DD45* (AT2G21740) and *INCURVATA2* (At5g67100) promoters were previously used for genome editing in Arabidopsis and might provide superior efficiencies or avoid the generation of chimeric mutant plants (Hyun *et al.* 2015, Mao *et al.* 2016, Wang *et al.* 2015). Additionally to kanamycin and BASTA selection, second generation recipients also allow for hygromycin selection, and contain a "fluorescence-accumulating seed technology" (FAST, Shimada *et al.* 2010) cassette in the T-DNA region. The FAST cassette mediates accumulation of RFP in the seed coat of various plant species, enabling for both positive and negative selection (Shimada*, et al.* 2010). Thus, non-transgenic seeds can be selected prior to screening (Gao *et al.* 2016) or once an intended lesion has been obtained to further simplify the selection of stable mutant lines from genome editing approaches. Second generation recipient vectors were developed as a possible enhancement of the pDGE series subsequent to first application. In the following, mainly first generation vectors will be used.

STRATEGIES AND EFFICIENCIES FOR ASSEMBLY OF RGN-CODING CONSTRUCTS

The exchange of the *ccdb* negative selection cassette in shuttle vectors and one step, one nuclease vectors for hybridized oligonucleotides by restriction/ligation (using *BpiI*, Figure 1b) takes place with high efficiency. Any negative clones obtained so far resulted from inaccuracies in oligonucleotide synthesis. Thus, vectors may also be used for screening applications in which libraries of unknown specificity nucleases are generated by cloning of degenerated guide sequences. Loaded shuttle vectors were used for the assembly of sgRNA arrays of different length in recipient vectors (Figure 1c). Efficiency of assembly reactions of two (M1 + M2E) or four (M1-3, M4E) sgRNA TUs was consistently above 90 %. The assembly efficiency of sgRNA arrays comprising eight TUs (M1-7,

M8E) was markedly decreased, but remained > 50%. Following a conservative cloning scheme (Figure S2a), constructs for expression of at least four sgRNAs can thus be assembled without any PCR steps in five days.

The high efficiencies of the Golden Gate assembly reactions, and the background-free cloning due to *ccdB*-mediated counter selection at all stages, prompted us to test polyclonal plasmid preparations for assembly (Figure S2b). Restriction/ligation reactions from loading shuttle vectors with hybridized oligonucleotides were transformed in *E. coli* and directly used for liquid cultures and plasmid isolation. Polyclonal plasmid preparations were used to assemble a construct with four different sgRNA TUs. No decrease in efficiency in comparison to a conservative assembly was observed. The "polyclonal" approach reduces time needed for the generation of a multiplexing construct by one day. More importantly, this strategy mitigates inaccuracies in oligonucleotide synthesis, as final assembly products will differ in incorporated oligonucleotide sequences. Furthermore, pooling of restriction/ligation reactions from loading sgRNA shuttle vectors prior to transformation into *E. coli* and polyclonal plasmid isolation was tested in a "fast track" assembly approach (Figure S2c). More than 50 % positive clones were obtained for assembly of an sgRNA array containing four TUs. However, the "fast track" approach is of limited use, as individual sgRNA modules may not be reused in different assemblies.

FUNCTIONAL VALIDATION OF NUCLEASE CONSTRUCTS AND EFFECTS OF SGRNA AND CAS9 DOSAGE

A "GUS-out-of-frame" recombination reporter was employed to test functionality of our genome editing toolkit. A spacer sequence was inserted in the coding sequence of a p35S-driven ß-glucuronidase (GUS), shifting the GUS gene out of frame. Introduction of DSBs within the reporter's spacer and subsequent repair by NHEJ should, in some cases, re-establish the reading frame of the GUS gene (Figure S3a). Thus, GUS activity upon co-expression of reporter and a respective nuclease can be used as a quantitative readout for nuclease activity. *Agrobacterium*-mediated transient expression of the GUS-out-of-frame reporter in *N. benthamiana* resulted in little to no GUS activity,

as expected (Figure S3b). Enhanced GUS activity was detected upon co-expression of the reporter with paired TALENs targeting the reporter's spacer (Figure S3b), suggesting that the GUS-out-of-frame reporter is suitable to monitor *in planta* nuclease activity.

Derivatives of pDGE62-65 and pDGE144-165 containing sgRNA1 (Table 1) for targeting of the reporter were transiently expressed, alone or in combination with the GUS-out-of-frame reporter, in *N. benthamina* leaf tissue. No or weak GUS activity was detected upon expression of RGNs or the reporter alone (Figure S4). Also, GUS activity did not exceed background level when Cas9 expression was driven by tissue-specific promoters (pDD45, pICU2). This suggests maintenance of expression patterns of these promoters in *N. benthamiana* transient assays. In contrast, strong GUS staining was obtained when Cas9 was expressed under control of the constitutive p35S and p*Pc*Ubi promoters in both vector sets (Figure S4). Thus, nucleases expressed from both one step, one nuclease and second generation recipient constructs are functional.

In planta nuclease activity might be limited by availability of Cas9 protein and/or sgRNA. A possible sgRNA dosage effect was tested by increasing copy number of sgRNA1 in derivatives of pDGE1 (p35S:Cas9). As a control, a nuclease construct containing eight copies of sgRNA6 (Table 1) targeting an *N. benthamiana* endogeneous locus was generated. In quantitative GUS measurements, low activity defining the background level was detected upon expression of either the nuclease containing eight sgRNA1 copies alone, the reporter alone, or the reporter together with the control nuclease containing sgRNA6 (Figure 2a). GUS activity was significantly enhanced upon co-expression of the reporter with a nuclease construct containing one copy of sgRNA1, as previously observed in qualitative GUS staining assays (Figures 2a, S4). With increasing sgRNA1 copy numbers, GUS activity was further enhanced (Figure 2a), suggesting that sgRNA abundance is one limiting factor for *in planta* nuclease activity at least in reporter-based assays. Furthermore, a respective sgRNA might be titrated out of the Cas9 complex by provision of additional sgRNAs in multiplexing applications. Nuclease constructs containing a single TU coding for sgRNA1, but additionally one, three or seven TUs coding for sgRNA6 were co-expressed with the GUS reporter (Figure 2a). GUS activity was not altered by expression of sgRNA6. The same constructs were tested in a reciprocal

experiment using a GUS reporter for sgRNA6 activity (Figure 2a, inset). GUS activity was enhanced upon co-expression of Cas9 and sgRNA6, and activity increased with sgRNA6 copy number, confirming activity of sgRNA6. Taken together, these results suggest that eight or more loci can be targeted in multiplexing applications without reduction of nuclease activity at a given target site. The functionality of sgRNAs expressed from different positions in an sgRNA array was tested by placing the reporter-targeting sgRNA1 at any possible position, while all other positions were occupied by sgRNA6 TUs (Figure 2b). A similar enhancement of GUS activity was measured upon co-expression of all nuclease constructs with the GUS reporter, indicating that any position within an sgRNA-TU array provides comparable genome editing activity. Finally, promoters for Cas9 expression were compared in quantitative nuclease activity assays (Figure 2c). Higher GUS activity and thus higher nuclease activity was obtained when using p2x35S in the *N. benthamiana* system. However, an amplification of nuclease activity by increasing sgRNA abundance was also detectable when using p*Pc*Ubi (Figure 2c). *In planta* nuclease activity is thus determined by both sgRNA and Cas9 abundance.

GENERATION OF CHROMOSOMAL DELETIONS IN *NICOTIANA BENTHAMIANA*

Stable, inheritable chromosomal deletions of ~50-100 bp were previously generated in tomato, and ~ 1 kb deletions were induced at the *ABP1* locus in Arabidopsis using Cas9-based nucleases (Brooks *et al.* 2014, Gao*, et al.* 2016). However, information for other species or about size biases for chromosomal deletions is to our knowledge so far missing. We made use of the simple and extensive multiplexing capacities of our genome editing toolkit to explore the generation of chromosomal deletions first in *N. benthamiana.* Three different nuclease constructs based on pDGE1 (p2x35S, nptII) and each containing four sgRNA TUs were generated. sgRNAs were designed for targeting of the immune regulatory genes *EDS1* and *PAD4. EDS1*-family genes additionally including *SAG101* encode essential regulators of plant innate immunity mediated by a subclass of nucleotide-binding/leucine-rich repeat- (NLR) type immune receptors containing an N-terminal Toll-Interleukin1-receptor (TIR) domain (Feys *et al.* 2001, Feys *et al.* 2005, Wagner *et al.* 2013). The *N. benthamiana* genome contains two plausible *EDS1* orthologues, which we termed *NbEDS1a* and

NbEDS1b (Table S2). In the following, only *NbEDS1a* will be analyzed. *Nb*PAD4 is encoded by a single gene (Table S2).

The four sgRNAs incorporated in each construct all targeted the same locus, and were designed two either generate small deletions (~ 100 bp) in pairs, or to generate larger deletions by cleavage of the outmost target sites (Figure 3a). Thus, the occurrence of small and large deletions can be analyzed in transformants originating from a single construct. pDGE30 (sgRNAs 2-5) targeted *NbEDS1*, while pDGE38 (sgRNAs 6-9) and pDGE80 (sgRNAs 10-13) targeted *NbPAD4* (Figure 3a, Table 1). Functionality of nucleases was first tested in transient expression experiments and using the amplified fragment length polymorphism (AFLP) assay (Belhaj*, et al.* 2013). The AFLP assay depends on detection of recombination products from paired nuclease activity by PCR using primers flanking the region targeted for deletion. Additional amplicons of the expected size were detected upon expression of pDGE30 and pDGE80 when querying for the generation of small deletions through cleavage of adjacent target sites (Figure 3b). On the same samples, no additional amplicons were detected when using outmost primers for detection. Activity of pDGE38 could not be detected.

Activity-confirmed nuclease constructs pDGE30 and pDGE80 were stably transformed into wild type *N. benthamiana.* Two independent plants transgenic for pDGE30 were genotyped for potential deletions. One plant apparently contained a deletion in exon 2 (Figure 3c), and band intensities suggested it was most likely heterozygous for the deletion. Sequencing of the smaller amplicon revealed that it corresponded to a 97 bp deletion in the second exon of *NbEDS1a* (*Nbeds1a-1*, Figure 3d). T_1 seedlings originating from the *Nbeds1a-1* candidate plant were genotyped, and the *Nbeds1a-1* deletion segregated as a Mendelian trait in this generation (Figure 3e). Upon transformation of pDGE80, 24 regenerated plants originating from 11 independent calli were obtained. None of the plants contained the deletion targeted by sgRNAs 12 and 13, but three independent transgenics homozygously carried a deletion in exon 2 of *NbPAD4* targeted by sgRNAs 10 and 11 (Figure 3f). Sequencing of amplicons revealed a bi-allelic deletion in plant 1 and a mono-allelic deletion in plant 4 (Figure 3g). T_1 seedlings were genotyped for two candidate homozygous deletion lines. The wild-type *NbPAD4* allele could not be detected, demonstrating that mutations were germline-transmitted.

Taking transformations of pDGE30 and pDGE80 together, 13 independent transgenic lines were genotyped. Although lines carrying small deletions could be recovered even in the homozygous state in T_0, as previously described for tomato (Brooks*, et al.* 2014), no line carrying a larger deletion by cleavage of external sgRNA targets was recovered. Since the functionality of all nucleases was shown via transient AFLP assays, this suggests reduced likelihood of larger deletions.

GENOME EDITING AT A COMPLEX *RESISTANCE* GENE LOCUS IN ARABIDOPSIS

The *DM2*^{Ler} (*Dangerous Mix 2*; Alcazar *et al.* 2009, Chae *et al.* 2014) *Resistance* gene cluster from accession Landsberg (L*er*) was chosen to exploit the generation of chromosomal deletions in Arabidopsis. *DM2*^{Ler} contains eight complete or truncated genes (*DM2a-DM2h*; Figure 4a) most homologous to *RPP1* conferring resistance to different isolates of the oomycete pathogen *Hyaloperonospora arabidopsidis* (*Hpa*) (Botella *et al.* 1998, Rehmany *et al.* 2005). When combined in a single genetic background with alleles of *Strubbelig Receptor Family 3* (*SRF3*) from accessions Kaschmir and Kondara, with a transgene encoding for nucleus-directed EDS1-YFP, or with an EMS-induced allele of the enzyme *O-acetylserine(thiol)lyase A1* (*OLD3*)*, old3-1, DM2*^{Ler} mediates temperature-dependent induction of autoimmune response (Alcazar *et al.* 2010, Stuttmann *et al.* 2016, Tahir *et al.* 2013). *old3-1*-induced autoimmunity leads to seedling lethality at ambient temperature (22°C), but is suppressed under high temperature conditions (Shirzadian-Khorramabad *et al.* 2010, Tahir*, et al.* 2013). *DM2*^{Ler} copy number strongly modulates *old3-1*-induced autoimmunity (our own observations, Shirzadian-Khorramabad*, et al.* 2010): Plants homozygous for *old3-1*, but hemizygous for *DM2*^{Ler} are viable at 22°C, but further reduction of growth temperatures (18°C) induces strong autoimmunity. This allows for phenotypic differentiation of heterozygous and homozygous *dm2* mutant plants using different temperature regimes.

Four different genome editing constructs for targeting of the *DM2* cluster were generated. pDGE142 (sgRNAs 22-25) and pDGE143 (sgRNAs 14-17) were based on pDGE4 (p*Pc*Ubi, BASTA) and designed to target two deletions each in *DM2c* and *DM2h*, respectively (Figure 4a, Table 1). Two

further constructs, pDGE89 and 90, were designed for deletion of the entire 120 kb region non-syntenic between Arabidopsis accessions Col and L*er* and containing the *DM2* cluster (Figure 4a). Constructs contained the same sgRNAs (18-21, Table 1), but differed in promoters driving Cas9 expression (p35S in pDGE89 or p*Pc*Ubi in pDGE90). sgRNAs for directing Cas9 to two sites at each flank of the targeted region were incorporated to potentially increase the frequency of large deletions (Figure 4a). Constructs were transformed into L*er old3-1* mutant plants, cultivated at 28°C to suppress *old3-1*-associated seedling lethality. T_1 transgenic plants were further BASTA-selected at 28°C, and propagated to obtain T_2 pools composed of five T_1 plants.

The *DM2h* locus necessary for mediating *old3-1*-induced autoimmunity (Stuttmann*, et al.* 2016) was targeted in pDGE143-transgenic plants. When cultivated at 22°C, approximately 5-10 % of T_2 seedlings were non-necrotic, representing candidate lines carrying at least one inactivating *dm2h* allele (Figure S5a). Further shifting plants to 18°C selected for homozygous *dm2h* mutant lines, which occurred at frequency < 10 % among the *dm2h* candidate lines (Figure S5a). BASTA was brush-applied to rosette leaves of surviving, putative homozygous *dm2h* candidate lines, and six BASTA-sensitive (non-transgenic) lines were genotyped. Only one of these contained a PCR-detectable deletion (between sgRNA 14 and 17 target sites, Figure 4b). An additional point mutational allele was sequenced, revealing a single nucleotide insertion (Figure 4b). Both *dm2h* lines were mono-allelic, indicating that mutations were most likely present in the T_1 germline, and became homozygous in the T_2 generation.

Survival at ambient temperatures was also used to screen for mutant lines containing a deletion encompassing the entire *DM2* cluster from T_2 pools transgenic for pDGE89 and pDGE90. Rescued seedlings were obtained at a frequency of ~ 0.5 % from pDGE90-derived, but not pDGE89-derived T_2 pools (Figure S5b). Four plants from different T_2 pools were randomly chosen for genotyping (Figure 4c). A PCR product corresponding to the deletion of the targeted 120 kb region was obtained in all cases, but differed in size. Sequencing revealed that size differences originated from either cleavage of the outer sgRNA18 and sgRNA21, or sgRNA19 and sgRNA21 targets (Figure 4d). Additional PCRs querying the presence of the wildtype $DM2^{Ler}$ locus showed that lesions were heterozygous in

deletion lines (Figure 4c, lower panel). Non-necrotic, putatively homozygous Δ*dm2* deletion lines were phenotypically isolated from segregating T_3 populations (Figure S5c), BASTA-sensitive individuals selected, and genotypes confirmed for two T_4 families (Figure 4e). Putative *dm2c* mutant lines were selected by PCR-screening approximately 150 pDGE142-transgenic T_2 plants cultivated under permissive conditions (28°C). No deletions from cleavage of sgRNA22/23 targets were obtained. However, lines containing a ~ 40 bp deletion derived from cleavage of sgRNA24/25 target sites were obtained at a frequency of 2.7 % in the homozygous state, and 8 % in the heterozygous state (Figure 4f). Again, transgene-free homozygous deletion lines were successfully selected in T_3, and molecular lesions were analyzed for two independent lines (Figure 3g). Both lines contained the PCR-selected, ~ 40 bp deletion, and also additional point mutations from cleavage of the sgRNA23 target site. Taken together, these results suggest that in Arabidopsis, i) point mutations occur with higher frequency than deletions targeted by paired nucleases, ii) Cas9-induced deletions mainly occur in T_2 when using p*Pc*Ubi:Cas9, iii) small deletions (here 40 bp) may occur at ~ 10 % frequency among T_2 plants, iv) relatively large chromosomal deletions (here 120 kb) are feasible, but occur at lower frequencies, and v) *Ubiquitin* Promoter-driven Cas9 appears more suitable than p35S-driven Cas9.

DELETION OF THE TANDEM *EDS1* LOCUS IN ARABIDOPSIS ACCESSION COL

The performance of p*Pc*Ubi:Cas9 in comparison to p35S:Cas9 was again tested using the *EDS1* locus as target. Accession Col contains two functional *EDS1* copies encoded by At3g48080 and At3g48090 (Figure 5a), and a Col *eds1-2* line was generated by introgression of the *eds1-2* allele from accession L*er* (Bartsch *et al.* 2006, Zhu *et al.* 2011). This line was instrumental for genetic analyses in the standard Col accession. However, it also contains the $DM2^{Ler}$ cluster, which may produce unexpected interference upon reestablishment of EDS1 activity in transgenic plants (Stuttmann*, et al.* 2016). The Col *EDS1* locus was targeted for deletion by two constructs containing sgRNAs 26-29 (Table 1), and either p35S-driven (pDGE91) or p*Pc*Ubi-driven (pDGE92) Cas9. Constructs were transformed into Col wild type plants, primary transformants selected by BASTA resistance, and fifteen T_2 pools corresponding to ~ 130 T_1 plants composed for each transformation. From T_2 pools, 60-70 seedlings

were screened for putative *eds1* mutant plants by infection with *Hpa* isolate Cala2. Resistance to *Hpa* Cala2 in Col is EDS1-dependent, and mediated by the TIR domain-containing immune receptors RPP2a/b (Sinapidou *et al.* 2004). None of the seedlings from transformation of pDGE91 (p35S:Cas9) was scored as *Hpa* Cala2 susceptible, but four plants from two independent pDGE92 T_2 pools were selected as potential *eds1* mutants. The expected ~ 5 kb deletion was detected in three *eds1* candidate lines (Figure 5b, upper panel). The wild type *EDS1* locus was not detected in lines containing the deletion, suggesting they were homozygous (Figure 5b, lower panel). Sequencing of deletion alleles from two *eds1* candidate lines revealed mono-allelic deletions encompassing the region flanked by sgRNA 26 and 28 target sites, while the sgRNA 29 target site remained intact in both lines (Figure 5c). A Col *eds1-12* mutant line not containing the pDGE92 transgene was selected in the T_3 generation, and seedlings were infected with *Hpa* Cala2 (Figure 5d). Col *eds1-12* seedlings were fully susceptible, and indistinguishable from the previously characterized Col *eds1-2* introgression line, confirming germline transmission of the deletion allele. With *eds1* being fully recessive, phenotypic screening for *Hpa* (Cala2) susceptibility fails to detect heterozygous deletion lines. From PCR-screening 230 individuals originating from six pDGE92 transformation-derived pools, either homo- or heterozygous deletion alleles were estimated to occur in ~ 10 % of T_2 (Figure 5e). However, actual frequencies might be lower, as stable, germline-transduced alleles may be confounded with somatic genome editing events occurring in leaf tissues used for DNA preparation. Taking deletions of the $DM2^{Ler}$ cluster and the tandem *EDS1* locus together, chromosomal deletions were obtained at two independent loci when using p*Pc*Ubi-driven Cas9, but not p35S-driven Cas9. Deletions apparently occurred at low frequencies in the T_1 generation, and became more frequent in T_2. Overall, the generation of chromosomal deletions not only provides a scheme for simple, PCR-based mutation identification, but also represents a feasible approach to overcome genetic redundancy or for functional dissection of non-coding DNA.

DISCUSSION

Strategies for assembly of RGN-coding constructs may include several PCR steps, combine different cloning strategies or rely on additional DNA modules such as destination vectors, thus adding variability and complexity (e.g. Lowder *et al.* 2015, Ma *et al.* 2015, Mao*, et al.* 2016, Zhang *et al.* 2015). The presented pDGE toolkit sacrifices some flexibility, but enables for extremely simple and fast assembly of RGN-coding constructs by Golden Gate cloning. Only hybridized oligonucleotides are required as "external" components, while all other DNA modules are part of the toolkit (Figure 1). Construction of second generation recipients showed how novel components and functionalities can be adapted for the "preassembled recipient" strategy (Figures 1 and S1). Arrays of two, four or eight sgRNA TUs may be assembled using sgRNA shuttle vectors. Arrays of different length can be constructed by providing suitable end-linkers in assembly reactions (Weber*, et al.* 2011a). A detailed manual for the assembly of RGN constructs is provided (Appendix S1), and plasmids can be obtained via Addgene (kit # 1000000084) or through us. Currently, functionality was only tested in *N. benthamiana* and Arabidopsis. However, functionality of p*At*U6 (for driving sgRNA expressions) as well as p*Pc*Ubi and p35S (for driving Cas9 expression) in many dicotyledonous plant species can be assumed.

We made use of the simple and efficient multiplexing capacity of our system to assemble multiple constructs incorporating four sgRNA TUs for the generation of chromosomal deletions. sgRNA target sites addressed by individual constructs were mostly chosen for the generation of either two small deletions by cleavage of nearby target sites, or larger deletions by cleavage of more distant target sites at the same locus (e.g. Figure 3a). In both *N. benthamiana* and Arabidopsis, mainly occurrence of small deletions (< 100 bp) was observed, and in only one case, more distant sites were cleaved to generate a large deletion (*dm2h-1*, Figure 4b). Also, phenotypically selected deletions of 5 kb (*AtEDS1*) and 120 kb (*AtDM2*) occurred at low frequencies (below 1 %), while small deletions were obtained at frequencies around 10 % (*AtDM2c*) by PCR-screening. Taken together, this suggests a reduction in the efficiency of deletion induction with increasing deletion size. However, a correlation between deletion size and frequency was not consistently observed in animal cells (Canver *et al.*

2014, He *et al.* 2015, Xiao *et al.* 2013), and frequencies might strongly depend on sgRNA activity rather than deletion size also in plant systems. In either case, the applied strategy of incorporating multiple sgRNAs in constructs for targeting of a single locus proved extremely valuable, as in most cases, only one of several possible deletions was obtained. Negative effects were not observed among Cas9-transgenic lines, indicating that unspecific cleavage at off-target sites is most likely not a major problem in plants. Thus, extensive multiplexing may not only be used for generation of higher order mutants, but also to increase mutation frequencies at single loci to reduce transformation and screening efforts.

Mainly point mutational alleles were obtained when phenotypically screening for inactivating alleles at the *DM2h* locus, corroborating lower frequencies of deletions in comparison to cleavage and repair events at single target sites. However, phenotypical selection is generally neither possible nor desired. In these cases, the induction especially of small chromosomal deletions provides a simple and straightforward workflow for the selection of mutant lines in genome editing approaches. Minor differences between wild type and deletion allele, as induced here at *NbEDS1a*, *NbPAD4* and *AtDM2c*, should generally not perturb PCR stoichiometry, and allow faithful selection of hetero- or homozygous deletion lines from simple PCR-screening. Confounding of recombination events occurring in populations of somatic cells with germline-transmitted alleles present in all cells only becomes problematic when targeting larger regions for deletion (Figure 5e). Deletion alleles are also convenient for downstream genetic analyses. Although high resolution melting analysis or dCAPS markers can be used to detect virtually any SNP in segregating populations, for example identification of an *N. benthamiana eds1 pad4* double mutant line, which was obtained at a frequency of 1/192 only, was simplified by the availability of size polymorphism markers for mutant alleles.

The RNA polymerase III (RNAP III)-transcribed U6/U3 promoter systems are most commonly used for the expression of sgRNAs in both animal and plant cells, as U6/U3 transcripts are not capped or polyA-tailed, are not exported from nuclei, transcription start sites are clearly defined, and a simple T stretch (≥ 6 Ts, Nielsen *et al.* 2013) is sufficient as termination signal. Our strategy for the expression of multiple sgRNAs consisted in repeated U6-driven TUs identical to each other with the exception of

the specificity-determining, variable guide sequence (Figure 1). Transient, recombination reporter-based assays indicated strong dependency of nuclease activity on sgRNA abundance, limited by the expression level of U6-driven sgRNAs (Figure 2a). However, it remains unclear whether nuclease activity at endogenous loci is similarly affected by sgRNA abundance. Also, limited nuclease activity might enhance Cas9-specificity (Fu *et al.* 2013, Hsu *et al.* 2013). Importantly, repetitive sgRNA expression units were not prone to silencing, as constructs were successfully used for the generation of multiple mutant lines, and mutations most likely occurred mainly in the T_2 generation in Arabidopsis. Thus, technically more demanding sgRNA expression systems bear valuable alternatives for specific applications as e.g. tissue-specific sgRNA expression (Gao and Zhao 2014, Nissim *et al.* 2014, Xie *et al.* 2015), but efficient multiplexing is also achieved by clustering sgRNA TUs. In reporter-based assays, 8 sgRNAs could be expressed without detectable reduction of nuclease activity at a given target site (Figure 2a), suggesting extensive multiplexing capacities also for the targeting of endogeneous loci.

Various RNAP II promoters were previously reported as functional for driving Cas9 expression in genome editing applications (e.g. Gao *et al.* 2015, Hyun*, et al.* 2015, Mao*, et al.* 2016, Wang*, et al.* 2015) (see Bortesi and Fischer 2015 for review). The 2x35S promoter was highly efficient in transient, reporter-based assays in comparison to the *Pc*Ubi promoter, and was also highly efficient for the generation of stable deletion mutants in *N. benthamiana* (Figures 2, 3). However, in two independent cases, deletion mutants could here be generated in Arabidopsis when using p*Pc*Ubi-driven, but not p35S-driven Cas9 in otherwise identical constructs. 35S:Cas9-mediated genome editing in Arabidopsis was previously reported (e.g. Feng *et al.* 2013, Jiang *et al.* 2014b), but direct comparison suggests reduced efficiency of this promoter. The egg cell-specific *DD45* promoter for driving Cas9 expression was recently reported to induce homozygous mutants at high frequency in the T_1 generation (Wang*, et al.* 2015), and was therefore incorporated in Cas9 units of second generation recipient vectors (Figure 1a). However, systematic comparison of promoters for Cas9 expression with unified target loci and selection schemes will be necessary to identify optimal Cas9 expression systems for genome editing in Arabidopsis in the future.

Besides sgRNA and Cas9 expression systems, choice of target sites and design of sgRNAs in perspective to the selection of mutant lines represent critical parameters for genome editing approaches. Among the 29 sgRNAs used in this study, we clearly observed differences in activity, with for example sgRNAs 10/11 efficiently inducing recombination events at the *NbPAD4* locus, but sgRNAs 6-9 not at all (Figure 3b). To date, no sgRNA design rules for plant systems are available, but predictive models for sgRNA on target efficiency were deduced in an animal system (Doench *et al.* 2016, Doench *et al.* 2014). Although with a limited dataset at hand, we considered whether design rules for highly efficient sgRNAs might explain variable nuclease activities observed here. Indeed, sgRNA pairs 6/7 and 8/9, for which no activity was detected, both contained an unfavorable target site (Table 1), and target sites for highly active sgRNAs 10/11 scored ≥ 0.3. However, sgRNA pair 2/3 and 4/5 targets also consistently obtained scores ≥ 0.3, but sgRNAs did not induce recombination with efficiencies comparable to sgRNA 10/11 (Table 1, Figure 3b). Also, sgRNA 28/29 target site scores were highly similar, but only cleavage of sgRNA28 was observed (Figure 5c). Thus, there is no strict correlation between high *in planta* activity and predicted activity. Future studies will help to confirm or define sgRNA design guidelines for plant systems, facilitating more informed target site selection.

EXPERIMENTAL PROCEDURES

Construction of pDGE1-4 vectors

Full lists of plasmids and oligonucleotides used in this study are provided in Tables S1 and S3. Annotated vector sequences are provided as multi-record genbank file in Appendix S2. If not further indicated, all pICH/pAGM/pICSL plasmids originate from the Plant Modular Cloning Toolbox (Engler*, et al.* 2014). *PAT* and *nptII* plant selectable marker cassettes were amplified from pAM-PAT (Genbank: AY436765.1) and pGWB5 (Nakagawa *et al.* 2007), respectively, using oligonucleotides JS584/688, and fragments cloned into pUC57-BsaI by *SmaI* cut/ligation, yielding pJOG32 (*PAT*) and pJOG33 (*nptII*). A *BsaI* recognition site within the *ccdB* gene of pDON207 (Invitrogen) was eliminated using JS691/692. The resulting derivative, pDON207-BsaI, was used as template to

amplify a *ccdB*-Cm^R (Cm^R – chloramphenicol resistance, *cat*) cassette using JS694/695. The resulting PCR product was cloned into pUC57-BsaI by *EcoRV* cut/ligation, yielding pJOG34. Golden Gate modules encompassing the Cas9 CDS (pICH41308::hCas9, Addgene #49770) as well as a 2xp35S:Cas9-tnos (pICH47742::2x35S-5'UTR-hCas9(STOP)-NOST, Addgene #49771) (Belhaj*, et al.* 2013) were obtained from Addgene. The parsley *Ubi4-2* promoter, p*Pc*Ubi (Fauser*, et al.* 2014), was amplified from parsley genomic DNA using JS834/835, and cloned into pICH41295 by *BpiI* cut/ligation, yielding pJOG20. p*Pc*Ubi (pJOG20), Cas9 (pICH41308::Cas9) and the *ocs* terminator (tocs, pICH41432) were combined in pICH47742 by *BsaI* cut/ligation, yielding pJOG30. pICH47742::2x35S-5'UTR-hCas9(STOP)-NOST, pJOG34 and either pJOG33 or pJOG32, and pJOG30, pJOG34 and either pJOG33 or pJOG32 were assembled in the pVM_BGW vector backbone (Schulze *et al.* 2012), a derivative of pBGWFS7 (Karimi *et al.* 2002), to create pDGE1-4, respectively. Assembly was carried out by *BsaI/BpiI* cut/ligation, followed by a cycle of ligation (Figure S1a), and a final digestion of the ligation reaction using *XbaI* to digest unincorporated pJOG34.

Construction of sgRNA shuttle vectors

A fragment encompassing the *At*U6 promoter, a guide sequence and the sgRNA scaffold was synthesized (Integrated DNA Technologies, Leuven, Belgium) and used for amplification *At*U6 promoter and sgRNA scaffold using oligonucleotides JS775/776 and JS779/780. A *ccdB*-CmR cassette was amplified using JS777/778 and pDON207-BsaI as template. The three PCR fragments were diluted, mixed and used as template for SOE PCRs for individual shuttle vectors using oligonucleotides indicated in Table S3. PCR products were cloned into pUC57-BsaI by *EcoRV* cut/ligation. To generate pDGE012 (M5), PCR fragments generated as previously using JS793/794 and generated with JS791/792 on Arabidopsis genomic DNA were fused by *BsaI* cut/ligation and used as template for PCR with JS791/794. The amplicon was cloned into pUC57-BsaI by *EcoRV* cut/ligation. To generate pDGE005 (M1), a linker sequence was amplified from Arabidopsis genomic DNA using JS781/782, the *At*U6 promoter was amplified using JS783/776, PCR fragments were

diluted, mixed as previously, used as template for PCR with JS781/784, and the amplicon was cloned into pUC57-BsaI by *EcoRV* cut/ligation.

Construction of pDGE62-65 vectors

A *BpiI* recognition site in pVM_BGW was mutagenized by amplification with JS704/705, followed by *BpiI* cut/ligation. The resulting pVM_BGW-BpiI backbone was used for assembly of pDGE62-65 from pICH47742::2x35S-5'UTR-hCas9(STOP)-NOST, pDGE006 and pJOG33 or pJOG32, and pJOG30, pDGE006 and either pJOG33 or pJOG32, respectively, by *BsaI/BpiI* cut/ligation, followed by a cycle of ligation and a final restriction with *XbaI*.

Construction of pDGE144-165

pJOG292 was constructed by combining the vector backbone (PCR JS1028/1029 on pVM_BGW-BpiI) and a *lacZ* fragment (PCR JS1030/1031 on pICH41264) in a *BsaI* cut/ligation reaction. A *ccdB* negative selection cassette (PCR JS1032/1033 on pDGE1) was subcloned into pUC57-BsaI by *EcoRV* cut/ligation. Promoter fragments were amplified from Arabidopsis DNA (DD45 – JS1074/1075; ICU2 – JS1055/1056) and cloned into pICH41295 by *BpiI* cut/ligation to yield pJOG301 and pJOG298, respectively. The Pro+5U modules were used for assembly of pJOG323 and pJOG326 in pICH47742. The FAST cassette from the Modular Cloning Plant Parts (Engler, et al. 2014) was used as level 1-3f module (pJOG304). pDGE144-165 were assembled by *BpiI* cut/ligation (Figure S1b).

Construction of pDGE76-79

Annealed oligonucleotides JS910/911 were used in a *BsaI/EcoRV* cut/ligation reaction with pICH41308::Cas9. After denaturing, the reaction was supplemented with fresh ATP, DTT, Ligase and *EcoRV* to obtain pJOG58. pJOG69 (2x35S:Cas9(D10A)-tnos) and pJOG70 (pPcUbi:Cas9(D10A)-

tocs) were assembled in pICH47742 with pJOG58, pICH51288, pICH41421, pJOG20 and pICH41432 by *BpiI* cut/ligation. pDGE76-79 were assembled from pJOG69/70 and pJOG32, pJOG33 and pJOG34 as described for pDGE1-4.

Construction of pJOG250-253

An N863A mutation was introduced into the Cas9 CDS in pJOG58, the insert amplified (JS912/913) and cloned into pAGM1287 by *BpiI* cut/ligation to yield pJOG60. A fragment coding for the C-terminus of Hax3 (AY993938) was amplified (oligonucleotides CTH3-GG-Jo-F/R) and subcloned into pPCR-Blunt, yielding pJOG241. pJOG242 was assembled from pJOG60, a Ser-Gly linker (oligonucleotides JS914/915 subcloned in pPCR-Blunt), pJOG241, pICH51277 and pICH41414 in pICH47742. pJOG250-251 and pJOG252-253 were constructed from pJOG242, pJOG32, pJOG33, pJOG34 and pDGE6 as described for pDGE1-4 and pDGE62-65, repectively.

Assembly of nuclease constructs

sgRNAs as indicated in Table1 were cloned into sgRNA shuttle vectors, and derivatives were subsequently used for assembly of nuclease constructs (pDGE30, 38, 80, 89-92, 142-143) as described in Appendix S1.

Construction of the GUS-out-of-frame recombination reporter and TALENs

The ß-glucuronidase coding sequence was amplified from pGWB3 (Nakagawa*, et al.* 2007) using oligonucleotides GUS_TALEN_Ax7LR-F and pTALENgus-R, and the resulting PCR product was cloned into pENTR/D TOPO (Thermo Fisher) as according to the manufacturer. The GUS-out-of-frame insert was subsequently mobilized into pGWB2 (Nakagawa*, et al.* 2007) by LR reaction, yielding pMR006. TALENs were assembled as previously described (Richter *et al.* 2014).

Agrobacterium-mediated expression, AFLP and GUS assay

Constructs were electroporated into *Agrobacterium* strain GV3101 pMP90 and grown on YEB media. For transient expression, plate-grown bacteria were resuspended (OD_{600} = -0.6) in Agro infiltration medium (AIM; 10 mM MES pH 5.7, 10 mM $MgCl_2$). Solutions were syringe-infiltrated. DNA was extracted by CTAB method at 3 dpi for AFLP assays. For qualitative GUS staining, leaf discs were collected 3 dpi, stained in GUS staining solution, destained with Ethanol, briefly rehydrated and dried in cellophane. For quantitative GUS assays, 2 leaf discs (9 mm diameter) were harvested per replicate, frozen in liquid nitrogen and lysed in a mixer mill. Tissue powder was resuspended in 300 µl GUS extraction buffer (50 mM NaH_2PO_4/Na_2HPO_4 pH7, 10 mM EDTA, 0.1 % SDS, 0.1 % Triton X-100) and samples cleared by centrifugation. 10 µl were mixed with 90 µl extraction buffer containing 5 mM 4-methylumbelliferyl-beta-D-glucuronide (4MUG), incubated for 1h, reactions stopped adding Na_2CO_3, and 4MU production measured on a Tecan Plate Reader against a series of 4MU standards. 4MU production was normalized against total protein amounts of the same samples determined by Bradford assay (Roti-Quant, Carl Roth) as according to the manufacturer.

Plant growth conditions and infection assays

N. benthamiana plants were cultivated in a greenhouse with 16 h light period, 60 % relative humidity at 24/20 °C (day/night). *A. thaliana* wild type accessions Columbia and Landsberg *erecta*, and the previously published L*er old3-1* (Tahir*, et al.* 2013) and Col *eds1-2* (Bartsch*, et al.* 2006) mutants were used. Arabidopsis plants were grown under short day conditions at 23/21 °C and with 60 % relative humidity or in a greenhouse under long day conditions. For suppression of autoimmunity, plants germinated under short day conditions (7d) before transfer to 28/26 °C (day/night). *Hpa* infection assays were done as previously described (Wagner*, et al.* 2013).

sgRNA design

CRISPR-P (Lei *et al.* 2014), CasOT (Xiao *et al.* 2014) and the sgRNA designer tool (Doench*, et al.* 2014) were used for selection of sgRNAs.

ACKNOWLEDGEMENTS

We thank Sylvestre Marillonnet, Nicola Patron and Vladimir Nekrasov and Sophien Kamoun for providing the Modular Cloning Toolkit (Addgene #1000000044), the Modular Cloning Plant Parts (Addgene #1000000047) and hCas9 modules (Addgene #49771 and #49770), respectively. Christine Wagner, Hannelore Espenhahn and Samuel Grimm are acknowledged for excellent technical assistance. This work and JO and JG were funded by a grant from the Deutsche Forschungsgemeinschaft to the Collaborative Research Centre (CRC) SFB 648. MR and JStr were supported by a grant from the Deutsche Forschungsgemeinschaft (BO 1496/8-1 to JB), a grant from the European Regional Development Fund of the European Commission to JB, and by the COST action FA1208 "SUSTAIN". The authors do not declare any conflict of interest.

SUPPLEMENTAL MATERIAL

Appendix S1: Manual for assembly of RGN-coding constructs using pDGE vectors

Appendix S2: Annotated vector sequences of pDGE vectors (multi-record genbank file)

Supplemental Table S1: Plasmids used in this study

Supplemental Table S2: Sequences of *N. benthamiana EDS1* and *PAD4* orthologues

Supplemental Table S3: Oligonucleotides used in this study

Supplemental Figure S1: Scheme for assembly of first and second generation recipient vectors

Supplemental Figure S2: Strategies and use of polyclonal DNA preparations for the assembly RGN-coding constructs

Supplemental Figure S3: Design and functionality of the GUS-out-of-frame recombination reporter

Supplemental Figure S4: Functional validation of one step, one nuclease and second generation recipient plasmids in transient reporter assays

Supplemental Figure S5: Phenotypic isolation of candidate *dm2h* and *dm2* mutant plants

REFERENCES

Alcazar, R., Garcia, A.V., Kronholm, I., de Meaux, J., Koornneef, M., Parker, J.E. and Reymond, M. (2010) Natural variation at Strubbelig Receptor Kinase 3 drives immune-triggered incompatibilities between Arabidopsis thaliana accessions. *Nat Genet*, **42**, 1135-1139.

Alcazar, R., Garcia, A.V., Parker, J.E. and Reymond, M. (2009) Incremental steps toward incompatibility revealed by Arabidopsis epistatic interactions modulating salicylic acid pathway activation. *Proceedings of the National Academy of Sciences of the United States of America*, **106**, 334-339.

Bartsch, M., Gobbato, E., Bednarek, P., Debey, S., Schultze, J.L., Bautor, J. and Parker, J.E. (2006) Salicylic acid-independent ENHANCED DISEASE SUSCEPTIBILITY1 signaling in Arabidopsis immunity and cell death is regulated by the monooxygenase FMO1 and the Nudix hydrolase NUDT7. *The Plant cell*, **18**, 1038-1051.

Belhaj, K., Chaparro-Garcia, A., Kamoun, S. and Nekrasov, V. (2013) Plant genome editing made easy: targeted mutagenesis in model and crop plants using the CRISPR/Cas system. *Plant methods*, **9**, 39.

Belhaj, K., Chaparro-Garcia, A., Kamoun, S., Patron, N.J. and Nekrasov, V. (2015) Editing plant genomes with CRISPR/Cas9. *Current opinion in biotechnology*, **32**, 76-84.

Boch, J. and Bonas, U. (2010) Xanthomonas AvrBs3 family-type III effectors: discovery and function. *Annu Rev Phytopathol*, **48**, 419-436.

Boch, J., Scholze, H., Schornack, S., Landgraf, A., Hahn, S., Kay, S., Lahaye, T., Nickstadt, A. and Bonas, U. (2009) Breaking the code of DNA binding specificity of TAL-type III effectors. *Science (New York, N.Y.*, **326**, 1509-1512.

Bortesi, L. and Fischer, R. (2015) The CRISPR/Cas9 system for plant genome editing and beyond. *Biotechnol Adv*, **33**, 41-52.

Botella, M.A., Parker, J.E., Frost, L.N., Bittner-Eddy, P.D., Beynon, J.L., Daniels, M.J., Holub, E.B. and Jones, J.D. (1998) Three genes of the Arabidopsis RPP1 complex resistance locus recognize distinct Peronospora parasitica avirulence determinants. *The Plant cell*, **10**, 1847-1860.

Brooks, C., Nekrasov, V., Lippman, Z.B. and Van Eck, J. (2014) Efficient gene editing in tomato in the first generation using the clustered regularly interspaced short palindromic repeats/CRISPR-associated9 system. *Plant physiology*, **166**, 1292-1297.

Canver, M.C., Bauer, D.E., Dass, A., Yien, Y.Y., Chung, J., Masuda, T., Maeda, T., Paw, B.H. and Orkin, S.H. (2014) Characterization of genomic deletion efficiency mediated by clustered regularly interspaced palindromic repeats (CRISPR)/Cas9 nuclease system in mammalian cells. *The Journal of biological chemistry*, **289**, 21312-21324.

Chae, E., Bomblies, K., Kim, S.T., Karelina, D., Zaidem, M., Ossowski, S., Martin-Pizarro, C., Laitinen, R.A., Rowan, B.A., Tenenboim, H., Lechner, S., Demar, M., Habring-Muller, A., Lanz, C., Ratsch, G. and Weigel, D. (2014) Species-wide genetic incompatibility analysis identifies immune genes as hot spots of deleterious epistasis. *Cell*, **159**, 1341-1351.

Christian, M., Cermak, T., Doyle, E.L., Schmidt, C., Zhang, F., Hummel, A., Bogdanove, A.J. and Voytas, D.F. (2010) Targeting DNA double-strand breaks with TAL effector nucleases. *Genetics*, **186**, 757-761.

Christian, M., Qi, Y., Zhang, Y. and Voytas, D.F. (2013) Targeted mutagenesis of Arabidopsis thaliana using engineered TAL effector nucleases. *G3 (Bethesda)*, **3**, 1697-1705.

Clasen, B.M., Stoddard, T.J., Luo, S., Demorest, Z.L., Li, J., Cedrone, F., Tibebu, R., Davison, S., Ray, E.E., Daulhac, A., Coffman, A., Yabandith, A., Retterath, A., Haun, W., Baltes, N.J., Mathis, L., Voytas, D.F. and Zhang, F. (2016) Improving cold storage and processing traits in potato through targeted gene knockout. *Plant Biotechnol J*, **14**, 169-176.

Doench, J.G., Fusi, N., Sullender, M., Hegde, M., Vaimberg, E.W., Donovan, K.F., Smith, I., Tothova, Z., Wilen, C., Orchard, R., Virgin, H.W., Listgarten, J. and Root, D.E. (2016) Optimized sgRNA design to maximize activity and minimize off-target effects of CRISPR-Cas9. *Nature biotechnology*, **34**, 184-191.

Doench, J.G., Hartenian, E., Graham, D.B., Tothova, Z., Hegde, M., Smith, I., Sullender, M., Ebert, B.L., Xavier, R.J. and Root, D.E. (2014) Rational design of highly active sgRNAs for CRISPR-Cas9-mediated gene inactivation. *Nature biotechnology*, **32**, 1262-1267.

Doudna, J.A. and Charpentier, E. (2014) Genome editing. The new frontier of genome engineering with CRISPR-Cas9. *Science (New York, N.Y*, **346**, 1258096.

Engler, C., Youles, M., Gruetzner, R., Ehnert, T.M., Werner, S., Jones, J.D., Patron, N.J. and Marillonnet, S. (2014) A Golden Gate Modular Cloning Toolbox for Plants. *ACS synthetic biology*.

Fauser, F., Schiml, S. and Puchta, H. (2014) Both CRISPR/Cas-based nucleases and nickases can be used efficiently for genome engineering in Arabidopsis thaliana. *Plant J*, **79**, 348-359.

Feng, Z., Zhang, B., Ding, W., Liu, X., Yang, D.L., Wei, P., Cao, F., Zhu, S., Zhang, F., Mao, Y. and Zhu, J.K. (2013) Efficient genome editing in plants using a CRISPR/Cas system. *Cell Res*, **23**, 1229-1232.

Feys, B.J., Moisan, L.J., Newman, M.A. and Parker, J.E. (2001) Direct interaction between the Arabidopsis disease resistance signaling proteins, EDS1 and PAD4. *EMBO Journal*, **20**, 5400-5411.

Feys, B.J., Wiermer, M., Bhat, R.A., Moisan, L.J., Medina-Escobar, N., Neu, C., Cabral, A. and Parker, J.E. (2005) Arabidopsis SENESCENCE-ASSOCIATED GENE101 stabilizes and signals within an ENHANCED DISEASE SUSCEPTIBILITY1 complex in plant innate immunity. *The Plant cell*, **17**, 2601-2613.

Fu, Y., Foden, J.A., Khayter, C., Maeder, M.L., Reyon, D., Joung, J.K. and Sander, J.D. (2013) High-frequency off-target mutagenesis induced by CRISPR-Cas nucleases in human cells. *Nature biotechnology*, **31**, 822-826.

Gao, X., Chen, J., Dai, X., Zhang, D. and Zhao, Y. (2016) An effective strategy for reliably isolating heritable and Cas9-free Arabidopsis mutants generated by CRISPR/Cas9-mediated genome editing. *Plant physiology*.

Gao, Y., Zhang, Y., Zhang, D., Dai, X., Estelle, M. and Zhao, Y. (2015) Auxin binding protein 1 (ABP1) is not required for either auxin signaling or Arabidopsis development. *Proceedings of the National Academy of Sciences of the United States of America*, **112**, 2275-2280.

Gao, Y. and Zhao, Y. (2014) Self-processing of ribozyme-flanked RNAs into guide RNAs in vitro and in vivo for CRISPR-mediated genome editing. *J Integr Plant Biol*, **56**, 343-349.

Geissler, R., Scholze, H., Hahn, S., Streubel, J., Bonas, U., Behrens, S.E. and Boch, J. (2011) Transcriptional activators of human genes with programmable DNA-specificity. *PLoS ONE*, **6**, e19509.

He, Z., Proudfoot, C., Mileham, A.J., McLaren, D.G., Whitelaw, C.B. and Lillico, S.G. (2015) Highly efficient targeted chromosome deletions using CRISPR/Cas9. *Biotechnol Bioeng*, **112**, 1060-1064.

Hsu, P.D., Scott, D.A., Weinstein, J.A., Ran, F.A., Konermann, S., Agarwala, V., Li, Y., Fine, E.J., Wu, X., Shalem, O., Cradick, T.J., Marraffini, L.A., Bao, G. and Zhang, F. (2013) DNA targeting specificity of RNA-guided Cas9 nucleases. *Nature biotechnology*, **31**, 827-832.

Hyun, Y., Kim, J., Cho, S.W., Choi, Y., Kim, J.S. and Coupland, G. (2015) Site-directed mutagenesis in Arabidopsis thaliana using dividing tissue-targeted RGEN of the CRISPR/Cas system to generate heritable null alleles. *Planta*, **241**, 271-284.

Jiang, W., Brueggeman, A.J., Horken, K.M., Plucinak, T.M. and Weeks, D.P. (2014a) Successful transient expression of Cas9 and single guide RNA genes in Chlamydomonas reinhardtii. *Eukaryotic cell*, **13**, 1465-1469.

Jiang, W., Yang, B. and Weeks, D.P. (2014b) Efficient CRISPR/Cas9-mediated gene editing in Arabidopsis thaliana and inheritance of modified genes in the T2 and T3 generations. *PLoS ONE*, **9**, e99225.

Jinek, M., Chylinski, K., Fonfara, I., Hauer, M., Doudna, J.A. and Charpentier, E. (2012) A programmable dual-RNA-guided DNA endonuclease in adaptive bacterial immunity. *Science (New York, N.Y*, **337**, 816-821.

Karimi, M., Inze, D. and Depicker, A. (2002) GATEWAY vectors for Agrobacterium-mediated plant transformation. *Trends in plant science*, **7**, 193-195.

Kim, Y.G., Cha, J. and Chandrasegaran, S. (1996) Hybrid restriction enzymes: zinc finger fusions to Fok I cleavage domain. *Proceedings of the National Academy of Sciences of the United States of America*, **93**, 1156-1160.

Lei, Y., Lu, L., Liu, H.Y., Li, S., Xing, F. and Chen, L.L. (2014) CRISPR-P: a web tool for synthetic single-guide RNA design of CRISPR-system in plants. *Mol Plant*, **7**, 1494-1496.

Liang, J., Chao, R., Abil, Z., Bao, Z. and Zhao, H. (2014) FairyTALE: a high-throughput TAL effector synthesis platform. *ACS synthetic biology*, **3**, 67-73.

Lowder, L.G., Zhang, D., Baltes, N.J., Paul, J.W., 3rd, Tang, X., Zheng, X., Voytas, D.F., Hsieh, T.F., Zhang, Y. and Qi, Y. (2015) A CRISPR/Cas9 Toolbox for Multiplexed Plant Genome Editing and Transcriptional Regulation. *Plant physiology*, **169**, 971-985.

Ma, X., Zhang, Q., Zhu, Q., Liu, W., Chen, Y., Qiu, R., Wang, B., Yang, Z., Li, H., Lin, Y., Xie, Y., Shen, R., Chen, S., Wang, Z., Chen, Y., Guo, J., Chen, L., Zhao, X., Dong, Z. and Liu, Y.G. (2015) A Robust CRISPR/Cas9 System for Convenient, High-Efficiency Multiplex Genome Editing in Monocot and Dicot Plants. *Mol Plant*, **8**, 1274-1284.

Mao, Y., Zhang, Z., Feng, Z., Wei, P., Zhang, H., Botella, J.R. and Zhu, J.K. (2016) Development of germ-line-specific CRISPR-Cas9 systems to improve the production of heritable gene modifications in Arabidopsis. *Plant Biotechnol J*, **14**, 519-532.

Nakagawa, T., Kurose, T., Hino, T., Tanaka, K., Kawamukai, M., Niwa, Y., Toyooka, K., Matsuoka, K., Jinbo, T. and Kimura, T. (2007) Development of series of gateway binary vectors, pGWBs, for realizing efficient construction of fusion genes for plant transformation. *J Biosci Bioeng*, **104**, 34-41.

Nielsen, S., Yuzenkova, Y. and Zenkin, N. (2013) Mechanism of eukaryotic RNA polymerase III transcription termination. *Science (New York, N.Y*, **340**, 1577-1580.

Nissim, L., Perli, S.D., Fridkin, A., Perez-Pinera, P. and Lu, T.K. (2014) Multiplexed and programmable regulation of gene networks with an integrated RNA and CRISPR/Cas toolkit in human cells. *Molecular cell*, **54**, 698-710.

Rehmany, A.P., Gordon, A., Rose, L.E., Allen, R.L., Armstrong, M.R., Whisson, S.C., Kamoun, S., Tyler, B.M., Birch, P.R.J. and Beynon, J.L. (2005) Differential recognition of highly divergent downy mildew avirulence gene alleles by RPP1 resistance genes from two Arabidopsis lines. *The Plant cell*, **17**, 1839-1850.

Richter, A., Streubel, J., Blucher, C., Szurek, B., Reschke, M., Grau, J. and Boch, J. (2014) A TAL effector repeat architecture for frameshift binding. *Nat Commun*, **5**, 3447.

Schiml, S., Fauser, F. and Puchta, H. (2014) The CRISPR/Cas system can be used as nuclease for in planta gene targeting and as paired nickases for directed mutagenesis in Arabidopsis resulting in heritable progeny. *Plant J*, **80**, 1139-1150.

Schulze, S., Kay, S., Buttner, D., Egler, M., Eschen-Lippold, L., Hause, G., Kruger, A., Lee, J., Muller, O., Scheel, D., Szczesny, R., Thieme, F. and Bonas, U. (2012) Analysis of new type III effectors from Xanthomonas uncovers XopB and XopS as suppressors of plant immunity. *New Phytol*, **195**, 894-911.

Shimada, T.L., Shimada, T. and Hara-Nishimura, I. (2010) A rapid and non-destructive screenable marker, FAST, for identifying transformed seeds of Arabidopsis thaliana. *Plant J*, **61**, 519-528.

Shirzadian-Khorramabad, R., Jing, H.C., Everts, G.E., Schippers, J.H., Hille, J. and Dijkwel, P.P. (2010) A mutation in the cytosolic O-acetylserine (thiol) lyase induces a genome-dependent early leaf death phenotype in Arabidopsis. *BMC plant biology*, **10**, 80.

Sinapidou, E., Williams, K., Nott, L., Bahkt, S., Tor, M., Crute, I., Bittner-Eddy, P. and Beynon, J. (2004) Two TIR:NB:LRR genes are required to specify resistance to Peronospora parasitica isolate Cala2 in Arabidopsis. *Plant J*, **38**, 898-909.

Sosso, D., Luo, D., Li, Q.B., Sasse, J., Yang, J., Gendrot, G., Suzuki, M., Koch, K.E., McCarty, D.R., Chourey, P.S., Rogowsky, P.M., Ross-Ibarra, J., Yang, B. and Frommer, W.B. (2015) Seed filling in domesticated maize and rice depends on SWEET-mediated hexose transport. *Nat Genet*, **47**, 1489-1493.

Stuttmann, J., Peine, N., Garcia, A.V., Wagner, C., Choudhury, S.R., Wang, Y., James, G.V., Griebel, T., Alcazar, R., Tsuda, K., Schneeberger, K. and Parker, J.E. (2016) Arabidopsis thaliana DM2h (R8) within the Landsberg RPP1-like Resistance Locus Underlies Three Different Cases of EDS1-Conditioned Autoimmunity. *PLoS Genet*, **12**, e1005990.

Tahir, J., Watanabe, M., Jing, H.C., Hunter, D.A., Tohge, T., Nunes-Nesi, A., Brotman, Y., Fernie, A.R., Hoefgen, R. and Dijkwel, P.P. (2013) Activation of R-mediated innate immunity and disease susceptibility is affected by mutations in a cytosolic O-acetylserine (thiol) lyase in Arabidopsis. *Plant J*, **73**, 118-130.

Townsend, J.A., Wright, D.A., Winfrey, R.J., Fu, F., Maeder, M.L., Joung, J.K. and Voytas, D.F. (2009) High-frequency modification of plant genes using engineered zinc-finger nucleases. *Nature*, **459**, 442-445.

Wagner, S., Stuttmann, J., Rietz, S., Guerois, R., Brunstein, E., Bautor, J., Niefind, K. and Parker, J.E. (2013) Structural basis for signaling by exclusive EDS1 heteromeric complexes with SAG101 or PAD4 in plant innate immunity. *Cell Host Microbe*, **14**, 619-630.

Wang, Z.P., Xing, H.L., Dong, L., Zhang, H.Y., Han, C.Y., Wang, X.C. and Chen, Q.J. (2015) Egg cell-specific promoter-controlled CRISPR/Cas9 efficiently generates homozygous mutants for multiple target genes in Arabidopsis in a single generation. *Genome biology*, **16**, 144.

Weber, E., Engler, C., Gruetzner, R., Werner, S. and Marillonnet, S. (2011a) A modular cloning system for standardized assembly of multigene constructs. *PLoS ONE*, **6**, e16765.

Weber, E., Gruetzner, R., Werner, S., Engler, C. and Marillonnet, S. (2011b) Assembly of designer TAL effectors by Golden Gate cloning. *PLoS ONE*, **6**, e19722.

Wiedenheft, B., Sternberg, S.H. and Doudna, J.A. (2012) RNA-guided genetic silencing systems in bacteria and archaea. *Nature*, **482**, 331-338.

Xiao, A., Cheng, Z., Kong, L., Zhu, Z., Lin, S., Gao, G. and Zhang, B. (2014) CasOT: a genome-wide Cas9/gRNA off-target searching tool. *Bioinformatics*.

Xiao, A., Wang, Z., Hu, Y., Wu, Y., Luo, Z., Yang, Z., Zu, Y., Li, W., Huang, P., Tong, X., Zhu, Z., Lin, S. and Zhang, B. (2013) Chromosomal deletions and inversions mediated by TALENs and CRISPR/Cas in zebrafish. *Nucleic Acids Res*, **41**, e141.

Xie, K., Minkenberg, B. and Yang, Y. (2015) Boosting CRISPR/Cas9 multiplex editing capability with the endogenous tRNA-processing system. *Proceedings of the National Academy of Sciences of the United States of America*, **112**, 3570-3575.

Zhang, Z., Mao, Y., Ha, S., Liu, W., Botella, J.R. and Zhu, J.K. (2015) A multiplex CRISPR/Cas9 platform for fast and efficient editing of multiple genes in Arabidopsis. *Plant cell reports*.

Zhu, S., Jeong, R.D., Venugopal, S.C., Lapchyk, L., Navarre, D., Kachroo, A. and Kachroo, P. (2011) SAG101 forms a ternary complex with EDS1 and PAD4 and is required for resistance signaling against turnip crinkle virus. *PLoS Pathog*, **7**, e1002318.

FIGURE LEGENDS

Figure 1: A toolkit for simple and efficient assembly of RGN-coding constructs

(a) Schemes of different types of pDGE vectors. Elements are not drawn to scale. sgRNA shuttle vectors differ in overhangs generated by restriction at flanking *BsaI* sites, as shown in a table next to the vector scheme.

(b) Principle for generating sgRNA TUs in either sgRNA shuttle vectors or one step, one nuclease vectors.

(c) Assembly of sgRNA TU arrays from loaded derivatives of shuttle vectors. Arrows in sgRNA arrays mark unique sequences, which can be used for final sequence verification.

Figure 2: Functional characterization of pDGE recipient plasmids in transient, reporter-based nuclease activity assays

(a) Effect of sgRNA dosage on *in planta* nuclease activity. Nuclease constructs containing varying copy numbers, as indicated, of reporter-targeting sgRNA1 or sgRNA6 (targeting an *N. benthamiana* endogenous locus) were co-expressed with the GUS-out-of-frame reporter in *N. benthamiana*. GUS activity was quantitatively determined at 3 dpi, normalized to total protein amounts, and expressed in relative units by arbitrarily setting GUS activity of the reporter alone to 1. Standard deviation of four biological replicates is shown, and letters indicate statistically significant differences (ANOVA, Tukey's Post-hoc test, $p < 0.01$). The

inset shows a reciprocal experiment, where the same constructs were co-expressed with a reporter targeted by sgRNA6.

(b) Functionality of sgRNA TUs within an sgRNA array. Nuclease constructs containing eight sgRNA TUs were expressed as in (a). Each construct contained seven copies of sgRNA6 and a single copy of sgRNA1. The position of sgRNA1 within the sgRNA array is indicated. Representation of GUS activity, replicates and statistics as in (a).

(c) Comparison of nuclease activity with different promoters driving Cas9 expression. Nuclease constructs with Cas9 expression driven by 2x35S or *Pc*Ubi4-2 promoters and containing either one or eight TUs for expression of the reporter-targeting sgRNA1 were expressed as in (a). Representation of GUS activity, replicates and statistics as in (a).

Figure 3: Generation of chromosomal deletions in *Nicotiana benthamiana*

(a) Schematic representations of the *NbEDS1a* and *NbPAD4* loci with oligonucleotides, sgRNA target sites and expected deletions indicated.

(b) Recombination events from nucleases activity detected by AFLP assay. Indicated constructs were transiently expressed in *N. benthamiana*, DNA extracted at 3 dpi and used as template for PCRs as indicated. Arrowheads mark additional PCR products from target site cleavage and recombination. Additional lanes were spliced in the right panel.

(c) Genotyping of two independent transgenic lines from stable transformation of pDGE30.

(d) Molecular lesion in the *Nbeds1a-1* deletion allele from (c).

(e) Segregation of the *Nbeds1a-1* deletion allele in T_1. A representative image from genotyping 20 T_1 individuals is shown with Chi^2 statistics.

(f) Genotyping of T_0 individuals from stable transformation of pDGE80. A representative image form genotyping in total 24 plants originating from 11 independent calli is shown.

(g) Molecular lesion in two *Nbpad4* deletion alleles from (f).

Figure 4: Generation of chromosomal deletions at the Arabidopsis *DM2* locus

(a) Schematic representation of the *DM2*^{Ler} locus with oligonucleotides and sgRNA target sites indicated. *R*-gene encoding *DM2a-h* genes are represented as dark grey arrows. A transposable element is indicated as a light grey box. Grey arrows mark loci conserved between Arabidopsis accessions Col and L*er* flanking the *DM2* locus, with numbers indicating Arabidopsis gene identifiers as At3gXXXXX.

(b) Molecular lesions detected in two phenotypically selected *dm2h* mutant lines (Figure S5a).

(c) Genotyping of phenotypically selected Δ*dm2* mutant lines (Figure S5b).

(d) Molecular lesions in two Δ*dm2* mutant lines.

(e) Genotyping of T_4 families for one Δ*dm2* mutant line, *dm2-2*. T_4 seedlings were pooled for DNA extraction, and DNAs were used for PCR with the indicated oligonucleotides.

(f) Genotyping of plants selected from a primary screen of approximately 150 T_2 plants from pDGE142 transformation.

(g) Molecular lesions in two *dm2c* mutant lines, as detected in single , BASTA-sensitive T_3 plants.

Figure 5: Deletion of the tandem *EDS1* locus in Arabidopsis accession Col

(a) Schematic representation of the *EDS1* locus with oligonucleotides and sgRNA targets indicated.

(b) Genotyping of phenotypically selected putative *eds1* deletion alleles. T_2 seedlings from transformation of pDGE92 into wild type Columbia plants were subjected to infection with incompatible *Hpa* isolate Cala2. Putatively *Hpa* susceptible, *eds1* candidate lines were used for DNA extraction and genotyping with indicated oligonucleotides.

(c) Molecular lesions obtained in *eds1* deletion alleles.

(d) Infection phenotype of the newly selected *eds1-12* mutant line and controls. Representative micrographs from infection with *Hpa* isolate Cala2 and staining of first true leaves with Trypan Blue (6 dpi) are shown. HR – hypersensitive response, fh – free hyphae.

(e) PCR-screening of T_2 plants as in (b) for *eds1* deletion mutants. Arrowheads mark signals interpreted as putative deletion lines.

Table 1: Sequences of target sites selected for this study

sgRNA#	**sequence [PAM]**	**target**	**pDGE***	**score****
sgRNA1	TATATAAACCCCCTCCAACC[AGG]	GUS Reporter	n/a	0.13
sgRNA2	GAAATTGGTCTGTTGATGGT[TGG]	*NbEDS1a* +	30	0.35
sgRNA3	AGCAAATGCTTCATTAACCA[TGG]	*NbEDS1b* (exon 1)	30	0.33
sgRNA4	ATCCCGGAATTATCAGCACG[AGG]	*NbEDS1a* +	30	0.60
sgRNA5	TATGCTGCATGTAATCTGAA[AGG]	*NbEDS1b* (exon 2)	30	0.44
sgRNA6	CGAAACGTTGGCAGCTTTTG[TGG]	*NbPAD4*	38	n/a***
sgRNA7	CACTTCGCCGTGATTAAAGT[TGG]	(exon 2)	38	0.32
sgRNA8	TTCACCAAGTTCTAGCCTCG[AGG]	*NbPAD4*	38	0.36
sgRNA9	TATAGAGATTAGAAGCTTCA[TGG]	(exon 3)	38	0.05
sgRNA10	GTTCGAGTCGAGCGAAACGT[TGG]	*NbPAD4*	80	0.80
sgRNA11	GGCGAAGTGGCTATCCACCG[AGG]	(exon 2)	80	0.30
sgRNA12	TCAGCTATTCCGCGTTGTGT[TGG]	*NbPAD4*	80	0.06
sgRNA13	CACTCTATCTGTGCTCTTAG[TGG]	(exon 3/4)	80	0.16
sgRNA14	AAATCTCACCGATACATGAA[AGG]	*DM2h* promoter	143	0.1
sgRNA15	TGATTTCTGCTAATTCATCA[AGG]	to exon 2	143	0.17
sgRNA16	ATTATACAGTTCAGTTACGA[TGG]	*DM2h* exon 3	143	0.21
sgRNA17	ATTATCAACCAAAGTGGAAG[AGG]		143	0.23

sgRNA18	TAACCGTCGGCTCGGGTCCT[TGG]	*DM2*^{Ler} left	89 & 90	0.01
sgRNA19	TGCGCCTTCGGATTCTCGGG[TGG]		89 & 90	0.57
sgRNA20	GTTAGGTCCTACGCAGTAAC[TGG]	*DM2*^{Ler} right	89 & 90	0.25
sgRNA21	CCACTGTTAGGCATGCATGA[TGG]		89 & 90	0.53
sgRNA22	CGGCTAAGCAATCTGATATG[TGG]	*DM2c* promoter	142	0.11
sgRNA23	TCCATTAGAATGGTGAAGGA[TGG]	to exon 1	142	0.16
sgRNA24	GGACAAAAGCACCCAAATGA[TGG]	*DM2c* exon 2	142	0.33
sgRNA25	AGGGAAGTTACCTACCTTGC[TGG]		142	0.03
sgRNA26	TGTCATCAGAATAGAGCCTG[AGG]	*AtEDS1* (Col) left	91 & 92	0.11
sgRNA27	GTATCCACGTGAGCGTATGA[TGG]		91 & 92	0.65
sgRNA28	CTGCGAAACTCCAGTCATGT[CGG]	*AtEDS1* (Col) right	91 & 92	0.31
sgRNA29	TTTGAGATGTCACTCTCGGT[TGG]		91 & 92	0.25

* pDGE construct containing respective sgRNA TUs

** On-target efficacy score of sgRNA, from 0 - 1, with 1 being best (Doench*, et al.* 2014).

*** Consecutive stretch of 4 Ts is not allowed by sgRNA designer tool

Figure 1 Ordon et al.

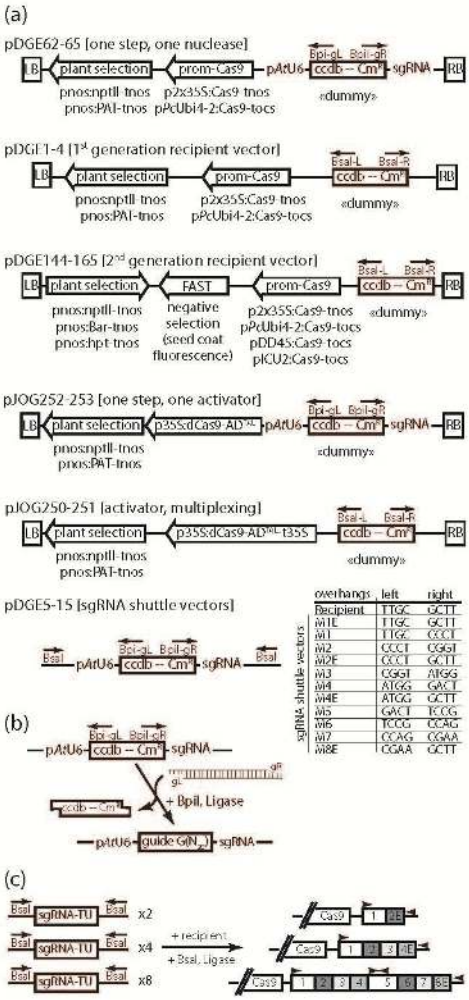

Figure 1: A toolkit for simple and efficient assembly of RGN-coding constructs

(a) Schemes of different types of pDGE vectors. Elements are not drawn to scale. sgRNA shuttle vectors differ in overhangs generated by restriction at flanking *BsaI* sites, as shown in a table next to the vector scheme.
(b) Principle for generating sgRNA TUs in either sgRNA shuttle vectors or one step, one nuclease vectors.
(c) Assembly of sgRNA TU arrays from loaded derivatives of shuttle vectors. Arrows in sgRNA arrays mark unique sequences, which can be used for final sequence verification.

Figure 2 Ordon et al.

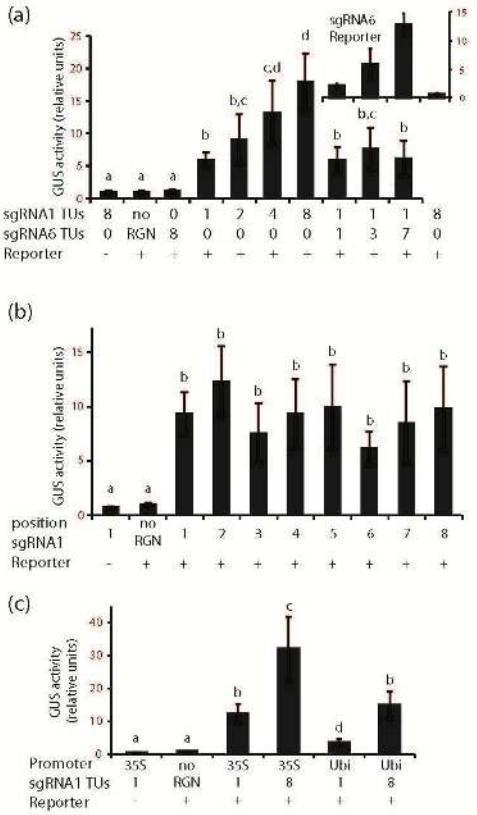

Figure 2: Functional characterization of pDGE recipient plasmids in transient, reporter-based nuclease activity assays

(a) Effect of sgRNA dosage on *in planta* nuclease activity. Nuclease constructs containing varying copy numbers, as indicated, of reporter-targeting sgRNA1 or sgRNA6 (targeting an *N. benthamiana* endogenous locus) were co-expressed with the GUS-out-of-frame reporter in *N. benthamiana*. GUS activity was quantitatively determined at 3 dpi, normalized to total protein amounts, and expressed in relative units by arbitrarily setting GUS activity of the reporter alone to 1. Standard deviation of four biological replicates is shown, and letters indicate statistically significant differences (ANOVA, Tukey's Post-hoc test, $p < 0.01$). The inset shows a reciprocal experiment, where the same constructs were co-expressed with a reporter targeted by sgRNA6.
(b) Functionality of sgRNA TUs within an sgRNA array. Nuclease constructs containing eight sgRNA TUs were expressed as in (a). Each construct contained seven copies of sgRNA6 and a single copy of sgRNA1. The position of sgRNA1 within the sgRNA array is indicated. Representation of GUS activity, replicates and statistics as in (a).
(c) Comparison of nuclease activity with different promoters driving Cas9 expression. Nuclease constructs with Cas9 expression driven by 2x35S or *Pc*Ubi4-2 promoters and containing either one or eight TUs for expression of the reporter-targeting sgRNA1 were expressed as in (a). Representation of GUS activity, replicates and statistics as in (a).

Figure 3 Ordon et al.

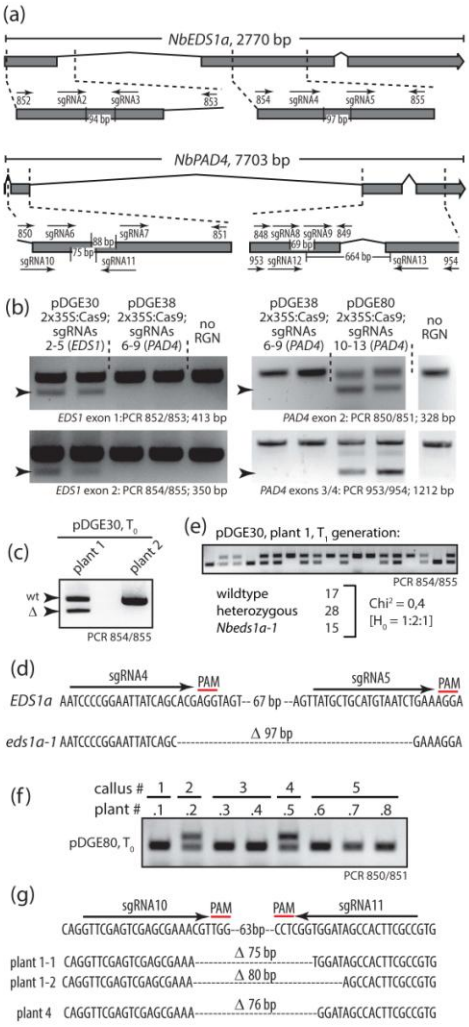

Figure 3: Generation of chromosomal deletions in *Nicotiana benthamiana*

(a) Schematic representations of the *NbEDS1a* and *NbPAD4* loci with oligonucleotides, sgRNA target sites and expected deletions indicated.
(b) Recombination events from nucleases activity detected by AFLP assay. Indicated constructs were transiently expressed in *N. benthamiana*, DNA extracted at 3 dpi and used as template for PCRs as indicated. Arrowheads mark additional PCR products from target site cleavage and recombination. Additional lanes were spliced in the right panel.
(c) Genotyping of two independent transgenic lines from stable transformation of pDGE30.
(d) Molecular lesion in the *Nbeds1a-1* deletion allele from (c).
(e) Segregation of the *Nbeds1a-1* deletion allele in T_1. A representative image from genotyping 20 T_1 individuals is shown with Chi^2 statistics.
(f) Genotyping of T_0 individuals from stable transformation of pDGE80. A representative image form genotyping in total 24 plants originating from 11 independent calli is shown.
(g) Molecular lesion in three *Nbpad4* deletion alleles from (f).

Figure 4 Ordon et al.

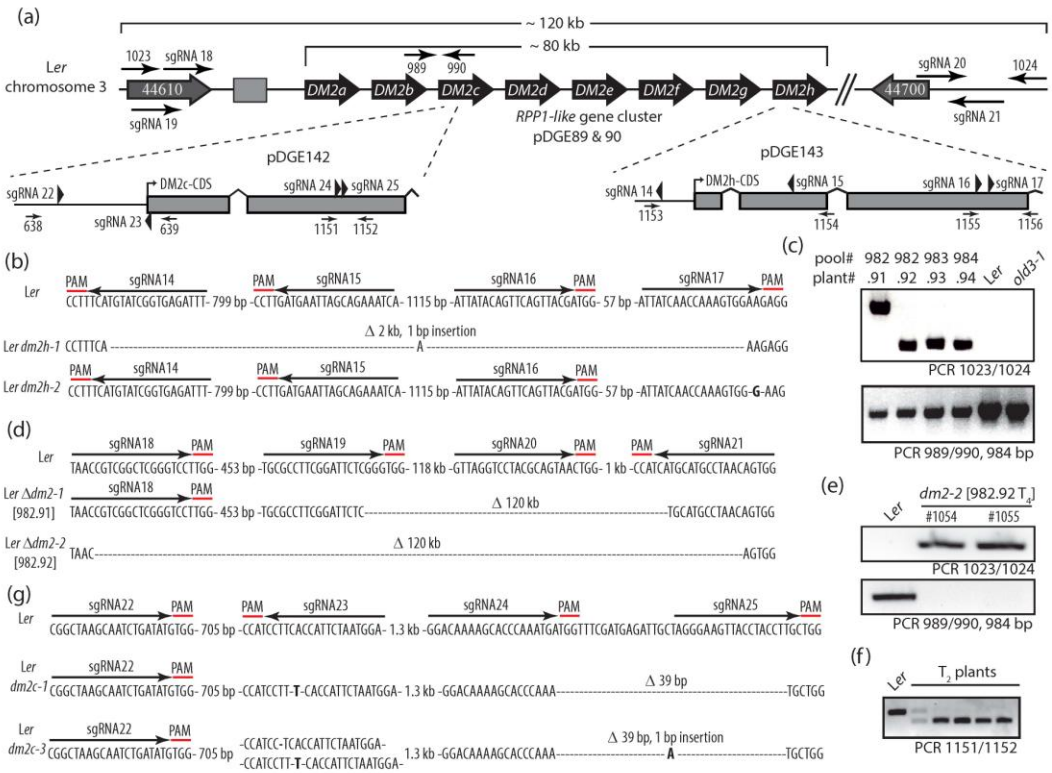

Figure 4: Generation of chromosomal deletions at the Arabidopsis *DM2* locus

(a) Schematic representation of the *DM2*^{Ler} locus with oligonucleotides and sgRNA target sites indicated. *R*-gene encoding *DM2a-h* genes are represented as dark grey arrows. A transposable element is indicated as a light grey box. Grey arrows mark loci conserved between Arabidopsis accessions Col and L*er* flanking the *DM2* locus, with numbers indicating Arabidopsis gene identifiers as At3gXXXXX.
(b) Molecular lesions detected in two phenotypically selected *dm2h* mutant lines (Figure S5a).
(c) Genotyping of phenotypically selected Δ*dm2* mutant lines (Figure S5b).
(d) Molecular lesions in two Δ*dm2* mutant lines.
(e) Genotyping of T_4 families for one Δ*dm2* mutant line, *dm2-2*. T_4 seedlings were pooled for DNA extraction, and DNAs were used for PCR with the indicated oligonucleotides.
(f) Genotyping of plants selected from a primary screen of approximately 150 T_2 plants from pDGE142 transformation.
(g) Molecular lesions in two *dm2c* mutant lines, as detected in single , BASTA-sensitive T_3 plants.

Figure 5 Ordon et al.

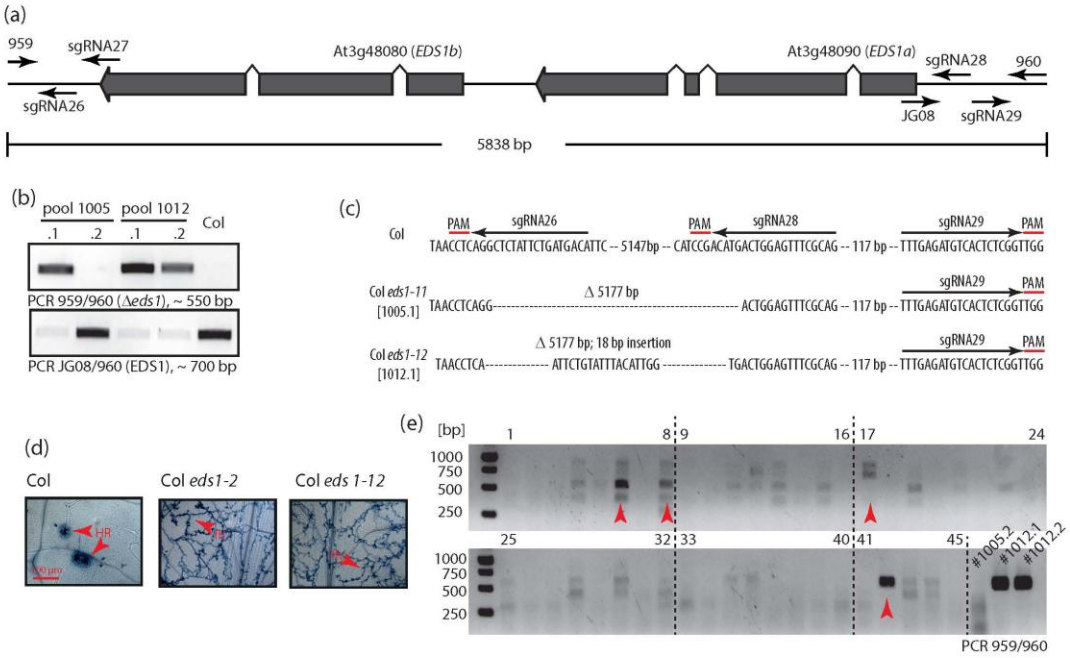

Figure 5: Deletion of the tandem *EDS1* locus in Arabidopsis accession Col

(a) Schematic representation of the *EDS1* locus with oligonucleotides and sgRNA targets indicated.
(b) Genotyping of phenotypically selected putative *eds1* deletion alleles. T_2 seedlings from transformation of pDGE92 into wild type Columbia plants were subjected to infection with incompatible *Hpa* isolate Cala2. Putatively *Hpa* susceptible, *eds1* candidate lines were used for DNA extraction and genotyping with indicated oligonucleotides.
(c) Molecular lesions obtained in *eds1* deletion alleles.
(d) Infection phenotype of the newly selected *eds1-12* mutant line and controls. Representative micrographs from infection with *Hpa* isolate Cala2 and staining of first true leaves with Trypan Blue (6 dpi) are shown. HR – hypersensitive response, fh – free hyphae.
(e) PCR-screening of T_2 plants as in (b) for *eds1* deletion mutants. Arrowheads mark signals interpreted as putative deletion lines.